Title
Pickoff and Transport of a 1 GeV Proton Beam from the Spallation Neutron Source to an ISOL Target

Author
Gough, R.A.

Publication Date
1998-09-01

ERNEST ORLANDO LAWRENCE
BERKELEY NATIONAL LABORATORY

Pickoff and Transport of a 1 GeV Proton Beam from the Spallation Neutron Source to an ISOL Target

R.A. Gough, J.G. Kalnins, and M.S. Zisman

Accelerator and Fusion Research Division

September 1998

LBNL-42311

Pickoff and Transport of a 1 GeV Proton Beam from the Spallation Neutron Source to an ISOL Target

R.A. Gough, J.G. Kalnins, and M.S. Zisman

Accelerator and Fusion Research Division
Ernest Orlando Lawrence Berkeley National Laboratory
University of California
Berkeley, California 94720

September 1998

This work was supported jointly by the Director, Office of Energy Research, Office of High Energy and Nuclear Physics, Division of Nuclear Physics, of the U.S. Department of Energy under Contract No. DE-AC03-76SF00098, and by the Physics Division of Oak Ridge National Laboratory.

Table of Contents

Pickoff and Transport of a 1 GeV Proton Beam from the Spallation Neutron Source to an ISOL Target[1]

September, 1998

1. Introduction

Critical to the success of an ISOL facility based on the Spallation Neutron Source (SNS) is a highly reliable and efficient method to separate and utilize a small, variable fraction ($\leq$10%) of the full energy beam from the SNS linac. As a guiding principle of this study, we recognize the need to accomplish this separation in a manner transparent to the neutron science program. This applies equally to the design, construction and operational phases of the SNS as well as the proposed future upgrades of the facility to higher power levels.

A schematic layout of the SNS is given in Fig. 1-1. This shows the control footprint of an upgraded facility incorporating two accumulator rings and two neutron-generating target systems. In the initial phase of the SNS, only one ring and one target station will be built and the total beam power will be 1 MW. An upgrade path has been identified to extend the performance of the facility first to 2 MW and subsequently to 4 MW; the second ring is needed in the upgrade from 2 to 4 MW. The shaded area at the top of the figure designates the space reserved for a future ISOL facility. It is assumed that the ISOL facility will be built concurrently with the initial construction phase of the SNS. Care will be taken to ensure that there is no interference between the ISOL facility and the second (future) SNS accumulator ring.

The SNS accelerates a beam of H^- ions to the full final energy of 1 GeV in a 60 Hz rf linac and delivers it via a high energy beam transport (HEBT) line to an accumulator ring for pulse compression and subsequent delivery of a short pulse to the target. At the end of the HEBT, the beam is converted to H^+ by passing it through a thin (~300 $\mu g/cm^2$) carbon stripper foil as it is injected into the ring. The proposed location for the ISOL pickoff is in the upstream portion of the HEBT, approximately 15 m downstream from the linac exit.

2. Description of SNS High Energy Beam Transport (HEBT) Line

The characteristics of the SNS beam and HEBT design are described fully in the SNS Design Manual, so only a brief description is provided here. The linac operates at 60 Hz and 6% duty factor. The H^- beam emerges from the linac in macropulses approximately 1 ms long with a 6% duty factor (see Fig. 2-1). The peak beam current is 28 mA for initial operation at 1 MW and will be increased to 56 mA during the upgrade to 2 MW. The beam is further chopped into mini-pulses at about a 1.2 MHz rate to provide a gap in the beam that circulates in the accumulator ring. (This gap is needed to accommodate the rise time of the fast kicker magnet in the ring extraction system.) These mini-pulses are created by a fast-chopper system located in the SNS front end. In addition, within each mini-pulse, there is a 402.5 MHz rf structure in the beam for SNS operating modes up to 2 MW. (This becomes 805 MHz following the upgrade to 4 MW, which utilizes interleaved beams from two front-end systems.)

---

[1]This report was prepared by Lawrence Berkeley National Laboratory for ORNL.

The layout of the SNS HEBT is shown in Fig. 2-2. The section most relevant to this study is the linac-to-achromat matching section (LAMS) of the HEBT, which transports the beam to the linac dump and to the 90 deg achromatic bend section. Dipole magnets in the HEBT are required to have a field strength less than 0.3 T to prevent losses due to Lorentz stripping. The LAMS section matches a lattice with a 19 deg phase advance in the linac to a 60 deg phase advance lattice in the achromatic bend section. This is accomplished using a quadrupole FODO lattice with 11.4 m cell length. Small, 0.2-m-long corrector magnets for beam steering are located immediately following each quadrupole. The first quadrupole, located at the linac exit, is horizontally focusing.

Twiss parameters for the horizontal (x) and vertical (y) planes at the center of the linac exit quad (QL0) are[2] $\beta_x = 16.33$ m, $\alpha_x = 0.318$, $\beta_y = 11.02$ m, and $\alpha_y = 0.303$, and the normalized rms emittance requirement at the end of the linac is 0.25 π mm-mrad. The optics parameters for the HEBT are shown in Fig. 2-3. These parameters describe a beam in the LAMS that is almost parallel, with the beam diameter varying slowly between approximately 6 and 9 mm. The quadrupole magnets (type 12Q50), spaced 5.7 m apart in the LAMS, have a 12 cm bore diameter, an effective length of 50 cm, and a maximum gradient of 4 T/m. Several cells in the downstream portion of the LAMS will incorporate halo scrapers to clean up the beam prior to injection into the ring. Minimizing uncontrolled beam loss is essential in the transport of the beam to avoid activation of beamline components. Some small (controlled) beam loss is unavoidable, for example in the halo scraper system. Beam position monitors and other beam diagnostics will be employed throughout the HEBT for beam tuning. During linac tune-up, the LAMS beamline will be used to guide the beam to the Linac Dump.

Through our interactions with the SNS project team, we have identified a specific location within the HEBT where a proton pickoff scheme could be implemented. This is in the third FODO half-cell downstream from the linac, between quadrupole QL2 and QL3. This location provides a roughly 5-m-long drift space between quadrupole magnets and allows enough room on the site layout to transport the proton beam to the ISOL target without interfering with the second accumulator ring (see Fig. 1-1). The presently planned pickoff point is also far enough upstream to avoid interference with the planned halo scrapers and other beam optics elements used to prepare the SNS beam for ring injection.

3. Proton Pickoff

There are several viable options that can meet the requirements for extracting a small and variable fraction of the 1 GeV SNS beam. As stated above, a guiding principle in this effort is to develop and implement an extraction scheme that will reliably serve the needs of the ISOL community without impacting the neutron science program. In this section we briefly discuss three possible approaches to this problem: a fast kicker magnet capable of cleanly deflecting up to 10% of the mini-pulses within the 1 ms macropulse; a Lorentz stripping scheme that would create a separable neutral beam of H^0 that could be subsequently stripped to H^+; and a stripper foil that would convert a variable fraction of the H^- beam directly to H^+. These three approaches are illustrated schematically in Figs. 3-1, 3-2, and 3-3, respectively. Based on our studies to date, we believe all three of these

[2]SNS Design Manual, DRAFT A, August 7, 1998.

approaches could be made to work; however, for reasons discussed below, we have based most of our efforts on the stripper-foil approach.

3.1 Fast Kicker

The first scheme (see Fig. 3-1) employs a fast kicker magnet capable of rising to full excitation in the 290 ns gap between mini-pulses, sustaining a field at (or close to) its full excitation for up to 100 μs, returning to zero field in $\leq$15 ms, and repeating this cycle at a 60 Hz repetition rate. The deflected beam from the kicker passes through a stripper foil converting it to H^+ (protons) and then into the extraction channel of a septum magnet which provides a complete separation from the axis of the H^- parent beam. An extra deflection could be achieved by arranging for the deflected beam to pass off-axis through a horizontally defocusing quad in the HEBT FODO lattice.

While the development of such a fast kicker magnet appears feasible with some R&D, we are unaware of any existing magnets that can meet these requirements. Traditional fast abort kickers used in modern synchrotrons are designed to dump the entire beam in a single revolution and do not employ power supply technology that can sustain full excitation of the magnet for 100 μs or operate at 60 Hz. Development of such a magnet is likely to be done in the future by the SNS facility as part of its upgrade to two accumulator rings, but this time frame is well after the proposed construction of the ISOL facility.

3.2 Magnetic Stripper

In the second scheme (see Fig. 3-2), the H^- beam passes through a short, high-field magnet that strips a variable fraction of the H^- beam to a neutral beam of H^0. The two beam components can then be separated by passing them through a magnet or system of magnets such as the chicane shown in Fig. 3-2. The undeflected H^0 beam is subsequently passed through a stripper foil converting it to protons that are then deflected away from the axis and directed into the ISOL transport line. A shielded beam stop is provided to safely collect the small residual beam of H^0. Because the initial stripping occurs continuously along the beam path within the stripping magnet, there is necessarily a distributed source for the proton beam. This leads to a proton beam with a higher emittance that must be transported to the ISOL target. A scheme based on this concept is in use at the LANSCE facility at Los Alamos National Laboratory to inject beam into the Proton Storage Ring (PSR). We are continuing to study and evaluate this approach to determine its cost, performance, and reliability.

3.3 Stripper Foil

In the third scheme, a stripper foil is used to convert a variable fraction of the beam to protons which can then be magnetically separated from the main H^- beam and directed into the ISOL transport line. We describe here a particular implementation of this concept (see Fig. 3-3) in which the H^- beam passes through a three-magnet chicane located between two of the quadrupole magnets that make up the FODO lattice of the LAMS beamline. In this arrangement, the three chicane dipoles operate below 0.3T, deflect the beam horizontally toward the left with a maximum displacement of about 7.5 cm and return it achromatically to the original axis. The first and third magnets are identical C-magnets that bend the beam through an angle $\theta = 2.5$ deg. They have an effective length of 90 cm . The middle dipole is an H-magnet with a 1.80 m effective length, and bends the beam through an angle $2\theta = \pm 5$ deg. A stripper foil with one unsupported edge is moved into the beam between the first and second magnets to intercept a variable fraction of the beam. The resulting proton beam is deflected an additional 5 deg toward the left as it passes through the second magnet and departs from the original axis at a total angle of 7.5 deg. The stripper foils can be mounted on a foil changing mechanism to permit replacement of foils without breaking vacuum.

At the SNS, carbon stripper foils approximately 300 μg/cm^2 thick will be used for injection stripping into the accumulator ring. The efficiency for conversion to protons in a carbon foil is determined by the following cross sections recently measured by Guley *et al.*:[3]

$$\begin{aligned}
\sigma_{-1,0} &= (6.76 \pm 0.09) \times 10^{-19}\ \text{cm}^2 \\
\sigma_{0,1} &= (2.64 \pm 0.05) \times 10^{-19}\ \text{cm}^2 \\
\sigma_{-1,1} &= (0.12 \pm 0.06) \times 10^{-19}\ \text{cm}^2
\end{aligned}$$

Using these cross sections, we have calculated the fraction of H^+, H^0 and H^- emerging from the carbon foil as a function of its thickness. The results are shown in Fig. 3-4. Beyond 200 μg/cm^2, the H^0 yield falls off exponentially, as seen in Fig. 3-5. For a foil thickness of 1 mg/cm^2, the H^0 fraction remaining is less than 1 part in 10^6 of the original beam. It is conceivable, however, that deterioration at the edge of the foil will result in an increase in H^0 production beyond acceptable levels, effectively limiting the foil lifetime. The energy deposited by a 1 GeV beam in a 1 mg/cm^2 carbon foil is less than 2 keV, so the peak power deposited in a foil intercepting 10% of the SNS beam is less than 6 W and the average power is less than 0.25 W. Even with this low power deposition, a thin carbon foil relies primarily on radiation to lose heat, and therefore will operate at a very high temperature. We investigated the possibility of using a metal foil, which can be manufactured down to 1 mg/cm^2 by roll forming. This will provide foils with a more robust edge and a much higher thermal conductivity. Beryllium foils, for example, have been manufactured this way and were used at the HILAC for many years. ANSYS calculations verify that the temperature of a 1 mg/cm^2 Be foil can be maintained below 300-400 °C, depending on the mounting design. This should provide a robust stripper foil with long life that will ensure that H^0 production remains acceptably low.

While it appears that several schemes for the proton pickoff can be made to work satisfactorily, we have focused attention on the stripper foil approach because of its low cost, simplicity and projected reliability. Other variants of this concept are also under evaluation. For example, a carbon fiber or series of carbon fibers could be used to strip from the center portion of the main beam.

[3]Gulley et al., Physical Review A 53, 3201 (1996).

4. Proton Transport to ISOL Target

4.1 Overview

The 215-m long ISOL proton transport system, referred to as LIBT (linac to ISOL beam transport) must accomplish several functions:

- Cleanly separate the 1 GeV proton beam from the SNS H^- beam
- Optically match to the SNS HEBT line in a transparent way
- Transport the proton beam out of the SNS tunnel to the ISOL target without interference with existing or planned SNS components
- Deliver the proton beam to one or more ISOL target stations.

As noted in Section 1, we require that the LIBT line have no impact on the ability of the SNS to operate in the event that it is unavailable. We also design it to accommodate a reasonable range of tuning to minimize the impact of changing the optics of SNS. Finally, to avoid possible disruption to SNS associated with the installation of the pickoff components of the LIBT, it is envisioned that these (see Section 5) will be fabricated early and installed simultaneously with the nearby SNS components.

To prepare the proton beam for ISOL, the H^- beam from the SNS linac must be stripped. The layout illustrated here is based on a stripping foil that intercepts about 10% of the primary beam. As discussed in Section 3, though other options have been considered, the stripping foil approach serves as our baseline design. The downstream optics system we propose, however, would be compatible with alternative stripping approaches as well. The LIBT comprises four optics "modules:" (1) Pickoff Achromat and Matching Section (PAMS); (2) Horizontal Achromat Section (HACS); (3) Vertical Achromat and Matching Section (VAMS); and (4) Target Switching Section (TASS). The overall layout is shown in Fig. 4-1. The 90% of the H^- beam not intercepted by the stripper foil is transported by the chicane magnets back to its original trajectory in the SNS LAMS line. We refer to the H^- portion of the PAMS optics, in effect part of the SNS HEBT system, as the Chicane to Achromat Matching Section (CAMS).

4.2 Pickoff Achromat and Matching Section (PAMS)

The PAMS is a horizontally achromatic section that serves to match the Twiss parameters at the SNS linac exit (QL0) to those at the entrance (QA1) to the HACS (see Section 4.3). It includes the chicane elements (see Fig. 4-2) that separate the protons from both the unstripped H^- and the small amount of neutral beam downstream from the foil and restore the unstripped beam back to its nominal trajectory in the SNS line. The restoration of the H^- beam also requires some minor optics rematching, as discussed below.

The chicane is made up of three dipoles, two C-magnets (MC1, MC3), and one H-magnet (MC2), whose parameters are summarized in Table 4-1. The first and third chicane dipoles, MC1 and MC3, are identical and bend the 1 GeV H^- beam by 2.5 deg. These magnets are designed with a field below 0.3 T to avoid Lorentz stripping of the beam. The stripping foil is situated between dipoles MC1 and MC2. The middle chicane magnet, MC2, has the same field but twice the length of MC1 and MC3, resulting in a 5-deg bend. As can be seen in Fig. 4-2, MC2 has opposite polarity to MC1 and serves to separate the stripped and unstripped beams. The proton beam is bent an additional 5 deg to the left, providing an overall angle of 7.5 deg from the linac beam axis. The unstripped beam is bent by –5 deg back toward the linac axis, giving it a net angle of –2.5 deg. This angle (as well as the dispersion it gives rise to) is removed by MC3, thus restoring the original H^- trajectory. The small amount of H^0 created in the stripping foil (see Section 3.3) will continue at +2.5 deg from the axis, passing close to quadrupole QL3 and stopping in a small shielded beam stop. (To provide clearance for the H^0 beam line, the HEBT/LAMS quadrupole QL3 will have to be modified or replaced by a C-type quadrupole.) Note that the pickoff chicane is contained entirely within the space between two HEBT quadrupoles (QL2 and QL3) and requires no change in the SNS focusing scheme aside from minor tuning adjustments to the first four LAMS quadrupoles (QL1, QL2, QL3, QL4) to account for the chicane dipole edge-focusing effect. Matching parameters are summarized in Table 4-2. The vacuum chamber in the chicane magnets will be designed to accommodate a straight-through trajectory for the H^- beam when all three chicane magnets are off. The beam envelope radius (x=horizontal; y=vertical) and dispersion for the CAMS section are shown in Fig. 4-3. This is for the nominal beam out of the CCL linac (i.e., unperturbed by the chicane stripper foil), with a horizontal and vertical transverse emittance value given in Table 4-3. Present estimates indicate that the emittance increase due to multiple scattering in the foil is small, below 10%.

Optics functions for the ISOL PAMS line are shown (together with the optics functions for the HACS line) in Fig. 4-4. Using the parameters in Table 4-3, a beam envelope below 7 mm results throughout. Magnet apertures are chosen to be compatible with SNS specifications to ensure minimal losses along the transport line. Note that the dispersion from MC1 and MC2 for the PAMS line is canceled downstream by dipole MP1 (see Table 4-4). Between MC2 and MP1 there is a quadrupole triplet (QP1, QP2, QP3) that serves mainly to ensure that the PAMS is achromatic. At the end of the PAMS, three quadrupoles (QP4, QP5, QP6) are used to match the Twiss parameters at QA1, the beginning of the HACS section. Collimators to clean up the beam after the stripping foil will be provided. The PAMS quadrupoles will be of the SNS 12Q50 design (12 cm bore aperture, 50 cm effective length) with the exception of the middle member of the triplet (QP2), which will have twice the length (i.e., a type 12Q100 or a pair of 12Q50 magnets in series). Corrector magnets based on the SNS design will be located at each quadrupole to permit steering of the transport line. Optics matching requirements for this section are summarized in Table 4-5.

Table 4-1. Chicane dipole parameters.

Designation	MC1, MC3	MC2
Type	C-magnet, rectangular	H-magnet, rectangular
Good field aperture [cm]	20	35
Gap [cm]	12	12
L_{eff} [m]	0.90	1.80
Bend radius [m]	20.6	20.6
Bend angle [deg]	2.5	±5
Edge angles (in, out) [deg]	0, 2.5	2.5, 2.5 (H^-) –2.5, 7.5 (H^+)
Field [T]	0.27	0.27

Table 4-2. Matching parameters for H^- beam in CAMS line.

	Entrance[a)]	Exit[b)]
Matching point location	QL0 midpoint (QF)	QL5 midpoint (QD)
β_x [m]	16.3	22.2
α_x	0.32	0
η_x [m]	0	0
η'_x	0	0
β_y [m]	11.0	10.0
α_y	0.30	0

a) Taken from Table 4.1-3, SNS Design Manual.

b) Beta functions estimated from data in the SNS Design Manual, using an average 45 deg phase advance per cell in the LAMS. Values will be modified as needed to reflect finalized SNS HEBT optics.

Table 4-3. Emittance and beam envelope parameters for H^- beam.

Normalized emittance, rms [π mm-mrad]	0.25
Unnormalized emittance, rms [π mm-mrad]	0.14
Envelope size	2.5σ

Table 4-4. PAMS dipole parameters.

Designation	MP1
Type	H-magnet, rectangular
Gap [cm]	12
L_{eff} [m]	1.0
Bend radius [m]	7.6
Bend angle [deg]	7.5
Edge angles (in, out) [deg]	3.75, 3.75
Field [T]	0.74

Table 4-5. Matching parameters for ISOL PAMS line.

	Entrance[a)]	Exit
Matching point location	QL2 midpoint (QF)	QA1 midpoint (QD)
β_x [m]	22.2	3.08
α_x	0	0
η_x [m]	0	0
η'_x	0	0
β_y [m]	10.0	14.6
α_y	0	0

a) Beta functions estimated from data in the SNS Design Manual, using an average 45 deg phase advance per cell in the LAMS. Values will be modified as needed to reflect finalized SNS HEBT optics.

4.3 Horizontal Achromat Section (HACS)

This section is used to transport the beam away from the linac tunnel and bend it horizontally by 150 deg toward the ISOL target area, at a trajectory chosen to avoid interference with the planned second SNS ring. The achromat is formed from four 9.74-m FODO cells having 90 deg phase advance per cell; optics functions, based on the emittance given in Table 4-3, are shown in Fig. 4-4. Quadrupoles are located midway between dipoles to give a symmetric FODO cell. Dipole magnet parameters are summarized in Table 4-6. In this portion of the LIBT, protons are being transported, so there is no restriction on the dipole field level. This permits a relatively compact line, with an average radius of only 15 m. For the quadrupoles, we have the option of using either the SNS 12Q50 or the 20Q50 type. The horizontal and vertical focusing quadrupoles will operate at essentially the same gradient of approximately 3 T/m. At the end of the HACS, the beam Twiss parameters are matched into the vertical bend region at the QV1 quadrupole. Corrector magnets based on the SNS design will be located at each quadrupole to permit steering of the beam in the transport line. Matching parameters are summarized in Table 4-7.

Table 4-6. HACS dipole magnet parameters.

	Dipole
Type	H-magnet
Gap[cm]	12
L_{eff} [m]	2.0
Bend radius [m]	6.1
Bend angle [deg]	18.75
Edge angles (in, out) [deg]	4.5, 4.5
Field [T]	0.93

Table 4-7. Matching parameters for ISOL HACS line.

	Entrance	Exit
Matching point location	QA1 midpoint (QD)	QV1 midpoint (QD)
β_x [m]	3.08	3.08
α_x	0	0
η_x [m]	0	0
η'_x	0	0
β_y [m]	14.6	14.6
α_y	0	0

4.4 Vertical Achromat and Matching Section (VAMS)

In this section the proton beam is transported vertically upwards from the elevation of the linac to the elevation of the target area. The nominal 6 deg vertical bending is done by two identical dipoles, MV1 and MV2, at each end of the VAMS. The FODO cell structure is similar to that of the LAMS portion of the SNS, with 60 deg phase advance per cell. Six cells are used to achieve the vertical achromat. As in other sections of the LIBT, quadrupoles, corrector magnets and beam diagnostics components identical to the SNS designs will be employed. The beam envelope and dispersion for the VAMS, along with the TASS (see Section 4.5), are shown in Fig. 4-5.

4.5 Target Switching Section (TASS)

The last section of the LIBT prepares the beam for delivery to the target. It is expected that several different target stations will ultimately be employed. Each may require a different optimization of beam size and aspect ratio on the target, and each line will have different dispersion, so the optics will need to be tailored accordingly. To focus the beam on target, we change from the FODO optics of the VAMS line to a quadrupole doublet scheme. The beam envelope and dispersion for the TASS are included in Fig. 4-5. The three quadrupole doublets smoothly transport and focus the beam at the target. This arrangement permits a range of spot sizes on target; a 5 mm diameter spot is shown. The switching magnet, MT1, will cover a range of 15 deg, and could run in either polarity. The present LIBT layout (shown in Fig. 4-1) has three target lines, at 0, 6.5, and 13 deg. The optics in Fig. 4-5 correspond to the central line (6.5 deg bend).

4.6 Component Designs

Many of the components required for the LIBT can be taken directly from the SNS designs with no modification. This applies to the quadrupoles, corrector magnets, and beam diagnostics devices. In the case of the quadrupoles, a few "special" magnets are envisioned. The central element in the PAMS triplet (QP2) is envisioned to have twice the length of the other quadrupoles. This could be accomplished in either of two ways—a longer magnet with the same transverse dimensions as the 12Q50 design could be built, or two 12Q50 quadrupoles could be placed close together and powered in series by a single supply. In the latter case, the magnets are not a design issue, but the power supply must be examined. Cost trade-offs have not been completed at this stage, but either approach is technically feasible. Similarly, the SNS LAMS quadrupole QL3, immediately downstream of the chicane magnets, must accommodate a straight-through line for the small H^0 intensity coming from the ISOL stripper foil. It may be possible to fit this line within the standard (or slightly modified) quadrupole outline, but this requires detailed layouts that have not yet been done. A straightforward alternative is to use a C-quadrupole at this location. A schematic cross section of such a magnet is shown in Fig. 4-6. Magnets of this type have been built for many synchrotron light sources, so their design is well understood. Quadrupole apertures will be kept large to be compatible with existing HEBT magnets and vacuum chambers (e.g., HEBT quadrupoles have a 12 cm aperture diameter).

In the case of the dipoles, special designs will be needed for the LIBT. Parameters for the chicane dipoles are summarized in Table 4-1. Those for the remaining horizontal dipoles are found in Tables 4-4 and 4-6. The vertical dipoles will be H-magnets similar to the MP1 dipole. They need provide about the same bend angle as MP1, however, so they could be either an identical design or a related design with a different length and different coils. Because the two vertical bends are identical, it is convenient to power them in series from a single supply. Dipole apertures will be kept large to be compatible with existing HEBT magnets and vacuum chambers (e.g., HEBT dipoles have an 8 cm gap). Low current densities will be maintained in the coils; HEBT magnets generally use <350 A/cm^2 wherever possible with up to 450 A/cm^2 used for some high field quadrupoles. A summary of the basic magnet design parameters is given in Table 4-8.

4.6.1 MC1 and MC3. As an initial design choice, we select a 12.1 cm magnet gap with 90 cm L_{eff} for the MC1 and MC3 C-type dipole magnets and a 180 cm L_{eff} for the MC2 H^-dipole (see Fig. 4-7 and Fig. 4-8). These effective lengths will result in a central field, B_0, of 0.27 T. Good field aperture widths will be approximately 20 cm for MC1 and MC3, and 35 cm for MC2 to allow for the variety of beam species (H^+, H^0 and H^-), and corresponding variety of beam trajectories, to be transported. The iron pole and core length will be assumed to be 80 cm and 170 cm for the 90 cm and 180 cm L_{eff} magnets, respectively, to account for the fringe field contribution to the integrated strength.

For convenience, we choose a standard LBNL copper conductor size with dimensions of 0.64 × 0.64-in. with a 0.402-in. diameter coolant passage hole (1.626 × 1.626 cm with 1.021-cm diameter hole). This conductor has an overall copper cross section of 0.281 in^2 (1.81 cm^2), a resistance of 29.6 (31.9) $\mu\Omega$/ft at 20 °C and 40 °C, respectively, and a conductor weight of 1.09 lbs/ft. Other conductor choices could easily be substituted, but our selection results in reasonable dimensions, power supply specifications, and operating conditions for the conceptual design. For a 0.27 T field and a 4.75-in. (12.1 cm) gap, the required ampere turns is given by NI = 2.02 × 4.75 × 2740 = 26,290 A-turns (assuming a magnetic efficiency very near 100% since these magnets operate at low field). Selecting two coils (one top and one bottom) with 20 turns each (say, 4 layers wide by 5 turns tall), the total current required would be 657 A and the current density would be 363 A/cm^2 (2338 A/in^2). (To provide some design margin, we specify and design the magnets for 0.3 T operation, requiring 720 A. Considerably more margin would be easily available if needed.)

In the coil package described above, each conductor occupies approximately 0.68 in. × 0.68-in. to account for insulating space between turns, with an additional 0.1-in. ground wrap and potting layer around the outer perimeter. Though the effective number of turns is 20, the coil package envelope allows for 6 turns (i.e., a 4 × 6 package) to allow for layer crossovers, transitions between layers, and coil-lead arrangements. Overall, we take the potted coil package to be 2.92-in. (7.4 cm) wide by 4.28-in. (10.9 cm) tall. We also provide a 2 cm clearance between the core ends and the coil, and 1 cm between the core leg/pole slot and coil.

The MC1 and MC3 cores will be fabricated out of low-carbon steel plate having good magnetic characteristics. To obtain a good field region 20 cm wide, we use an overall pole width of 36 cm (allowing for pole edge shimming, etc.). The pole length is 80 cm (resulting in 90 cm L_{eff}). The net flux entering the poletip is assumed to be 0.3 T entering over an effective area of L_{eff} by W_{eff}, or 90 cm × 46 cm. We wish to design the leg of the magnet to operate at about 1 T so, for an 80 cm long leg, the width/thickness of the leg must be about 15.5 cm, or 6.1 in. A nominal 6-in. thick plate will thus be used for the leg (and also the nominal top and bottom yoke thickness); the field resulting level will be approximately 1.02 T.

The mean coil length per turn is $2 \times 34 + 2 \times 80 + 2\pi \times 6 = 266$ cm (8.73 ft). The total magnet conductor length required for two 20-turn coils is 349.1 ft. The total resistance would be $R = 0.01114$ ohms at 40 °C. The voltage would be $720 \times R = 8.02$ V, and the power would be $720 \times V = 5.77$ kW for the entire magnet. With both circuits cooled in series, we would need $Q=3.8P/20$ for $\Delta T = 20$ °C, i.e., 1.1 gpm total flow. To get this flow through 350 ft of 0.402-in. diameter tube, a pressure drop of only about 21 psi is required. This is easily achievable; much higher actual flow rates will likely be realized. During an optimization design cycle, smaller conductor sizes with lower currents (and higher voltages) will also be considered, but the overall cross section coil envelope size will remain approximately the same.

4.6.2 MC2. For a good field region 35 cm wide, we take an overall pole width of 51 cm (see Fig. 4-8). The poletip length is assumed to be 170 cm (resulting in 180 cm L_{eff}). The net flux entering the poletip is 0.3 T entering over an effective area of 180 cm × 61 cm. If we wish to design the leg of the magnet to operate at about 1 T, and we assume it is also 170 cm long, then the width/thickness of each leg should be about 9.7 cm, or 3.8-in. With a nominal 4-in. thick plate for both legs (and also nominal top and bottom yoke thickness), the field level would be approximately 0.95 T.

The mean coil length would be $2 \times 49 + 2 \times 170 + 2\pi \times 6 = 476$ cm (15.6 ft). The magnet conductor length for each coil (for 20 turns) is 312.1 ft. At 40 °C, the resistance for each coil would be 0.00996 ohms, the voltage would be $720 \times R$, or 7.17 V, and the power would be $720 \times V$, or 5.16 kW for each coil. For the complete magnet (both coils), the resistance would be 0.0199 ohms, the voltage would be 14.34 V and the power would be 10.32 kW. If we cool each coil separately (two cooling circuits for the magnet), we would need $Q=3.8P/20$ for a 20 °C temp rise, or 1.0 gpm total flow for each coil, (2 gpm for the entire magnet). To achieve 1.0 gpm through 312 ft of 0.402-in. diameter tube, a pressure drop of about 20 psi would be required. For the entire MC2 magnet, a total flow of 2 gpm should be planned. This is easily achievable; much higher actual flow rates will likely be realized. During the optimization design cycle, smaller conductor sizes with lower currents (and higher voltages) will be considered, but the overall coil envelope cross section will remain approximately the same.

Table 4-8. Summary of basic chicane magnet parameters.

Parameter	Magnet		
	MC1	MC2	MC3
Type	C-type	H-type	C-type
Good field aperture [cm]	20	35	20
Gap (cm)	12	12	12
Design Field [T]	0.3	0.3	0.3
L_{eff} [cm]	90	180	90
Core dim: $L \times W \times H$ [cm]	$80 \times 61 \times 69$	$170 \times 89.8 \times 58$	$80 \times 61 \times 69$
Weight [kg]	2,257	5,435	2,257
Iron [kg]	2,085	5,114	2,085
Copper [kg]	172	321	172
Current [A]	720	720	720
Voltage [V]	8	14.3	8
Power [kW]	5.8	10.3	5.8
Coil $W \times H$ [cm]	7.4×11	7.4×11	7.4×11
No. of coils	2	2	2
Turns/coil	20	20	20
Matrix array	4 x 5	4 x 5	4 x 5
Conductor	0.64" sq. hollow Cu	0.64" sq. hollow Cu	0.64" sq. hollow Cu
Cur. density (A/cm^2)	398	398	398

5. Cost Summary for Early Design/Fabrication/Installation of Proton Pickoff Components

5.1 Rationale for Choices

The most important reason to install some of the key components of the proton pickoff line early is that subsequent installation (i.e. after the SNS HEBT has been installed) would lead to a significant interruption of the SNS program. In the chicane region, the spacing between components is very tight, and the two beamlines (SNS LAMS and ISOL PAMS) share a common vacuum chamber. This means that the required vacuum equipment and diagnostics devices must be available for initial SNS installation. Moreover, it is intended that the three PAMS chicane magnets (MC1, MC2, MC3) become part of the LAMS line optics. As such, they must be available on Day 1 of SNS operation. It is likely that common supports and alignment mechanisms will be needed for some components due to the spatial constraints. These are best designed concurrently by the engineering team.

Similarly, whatever modifications to quadrupole QL3 are required to handle the small neutral beam coming from the ISOL stripping foil must be made initially, so that the magnet used by the SNS beam is the "final" version.

As noted below, we cover here only the technical components. Modifications to the tunnel to permit a stub line directed toward the ISOL facility must also be done as part of the initial civil construction.

5.2 Scope

The following pre conceptual estimates cover the early design, fabrication and installation of those technical elements of the proton pickoff system that interface directly to the SNS HEBT beamline. It is assumed that these systems would be installed and made operational simultaneously with the SNS construction of the HEBT conventional facilities and the HEBT technical systems. Estimates below include costs for ED&I, procurement and/or fabrication, and installation at the SNS site. Not included in this estimate are the costs associated with conventional construction (stub-out tunnel, buildings, utilities, wireways, vents, power cabling into the tunnel, etc.). Also not included are the foil stripper assembly and the proton transport line elements beyond the MC2 magnet.

Table 5-1. Cost estimate (FY98 dollars) for ISOL early installation components.

Dipole magnet systems		$500K
	MC1, MC2, MC3	
	Power supplies	
	Interlocks	
	Support stands	
	Survey and alignment	
Quadrupole magnet		$75K
	Special QL3 quadrupole magnet	
	(Power supply and supports from SNS)	
Vacuum Systems		$250K
	Special vacuum chambers	
	Pumps	
	Valves/blank-offs	
Diagnostics		$50K
Subtotal		$875K
Contingency @ 37%		$325K
TOTAL		$1,200K

5.3 Discussion of Costs

In general, the items required for early installation are components typical of any synchrotron facility and, as such, their costs can be estimated with reasonably good accuracy even in the absence of a detailed engineering design. The estimates in Table 5-1 come from pre-conceptual designs for the devices listed, or from typical costs for like items known to an experienced accelerator engineer. In view of the preliminary state of the design, a somewhat higher contingency has been applied to the costs.

6.0 Acknowledgment:

The authors are pleased to acknowledge the support and guidance from Fred Bertrand and Jerry Garrett at Oak Ridge National Laboratory. We also gratefully acknowledge engineering support from from Missy Ogan (ORNL) for help with the civil construction aspects of the proposed ISOL facility, and from Ron Yourd, Kurt Kennedy and Daryl Oshatz (LBNL) for their help with magnet design and stripper foil calculations.

List of Illustrations

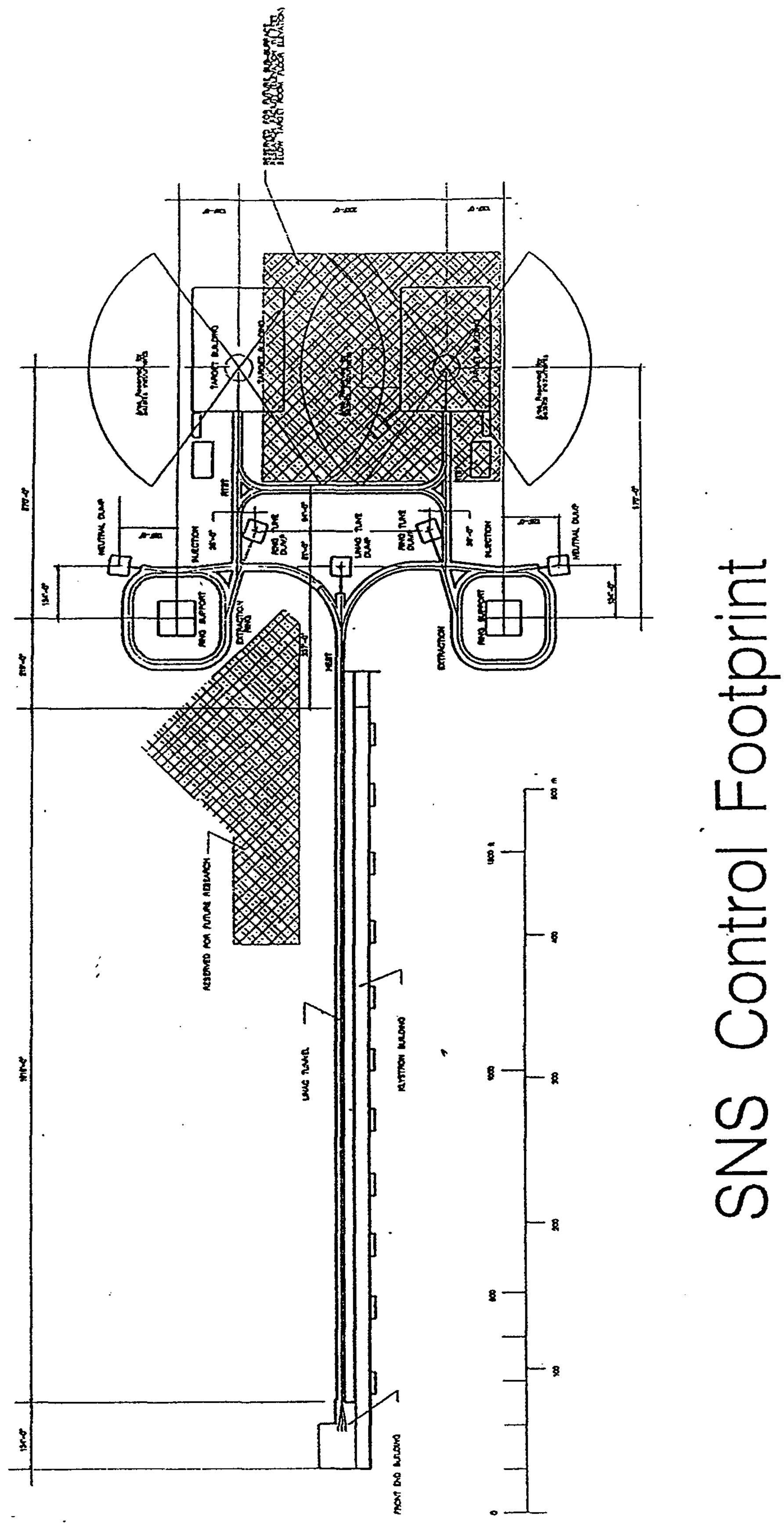

Figure 1-1. SNS control footprint showing the facility after the upgrade to two accumulator rings.

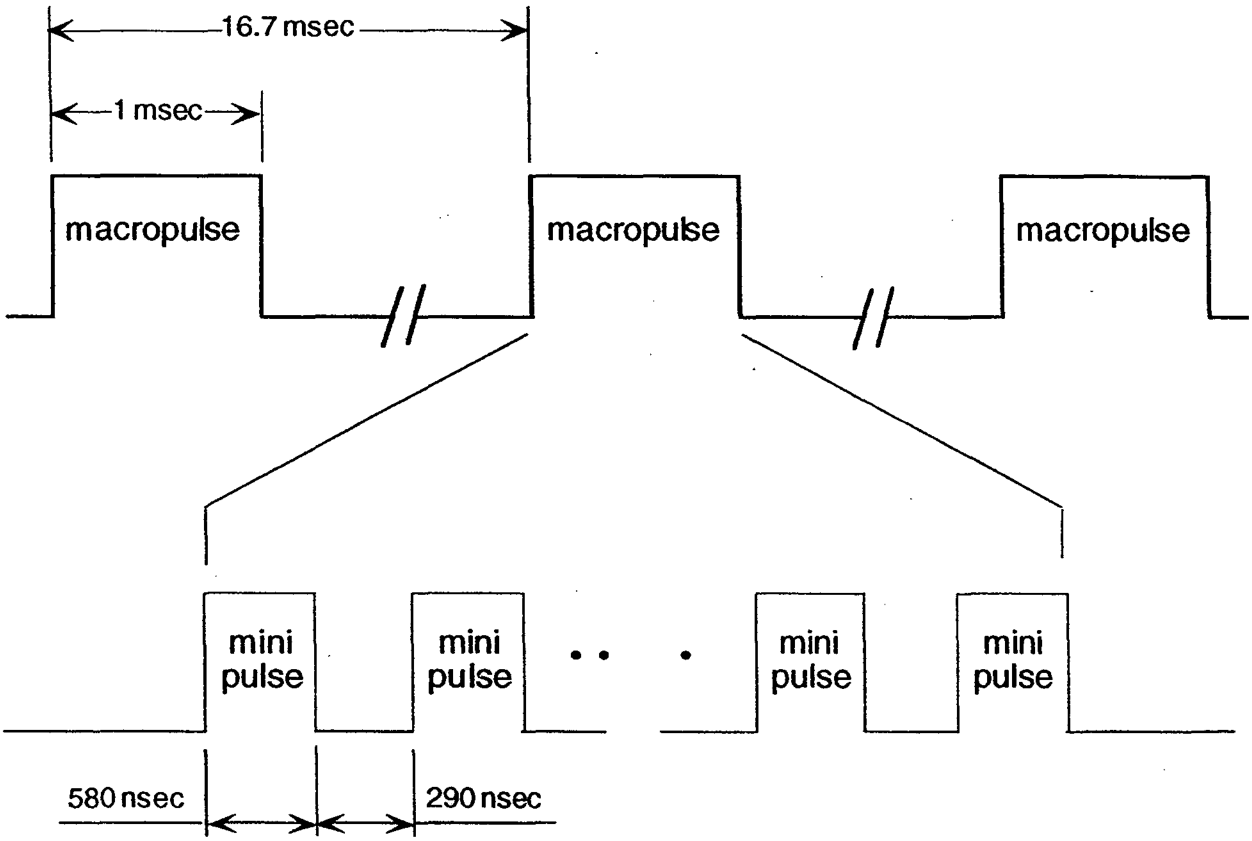

Figure 2-1. Pulse structure of the SNS beam.

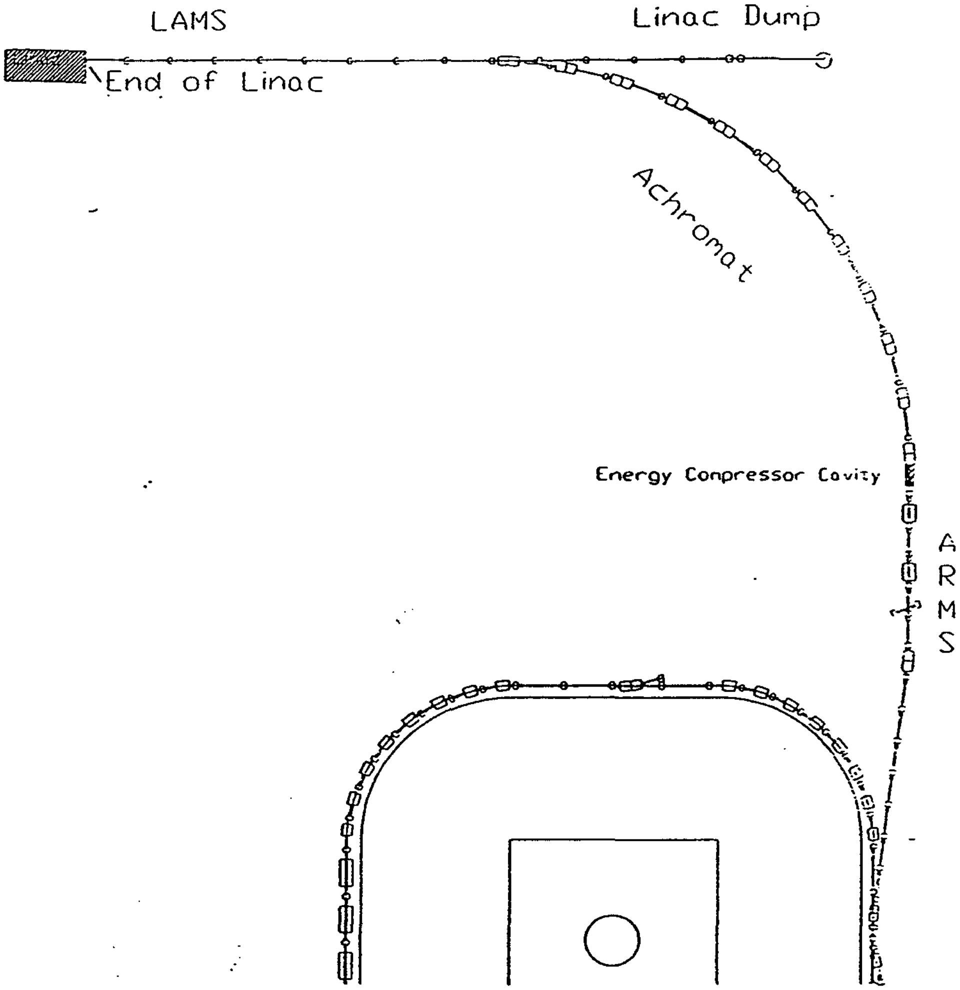

Layout of the HEBT line.

Component specifications for the HEBT

	Type	Location	No.	Field	Aperture	Length
Dipoles	7.5°	Achromat	12	0.3 T	8 cm gap	2.5
	7.5°	ARMS	1	0.3 T	8 cm gap	2.5
	Corrector	LAMS, ARMS	21	0.03 T	12 cm × 12 cm	0.2 m
	Corrector	Achromat	12	0.03 T	20 cm × 20 cm	0.2
Quadrupoles	QF/QD	LAMS, ARMS	21	4 T/m	12 cm ϕ	0.5 m
	QF/QD	Achromat	12	4 T/m	20 cm ϕ	0.5
E Compressor	16 cell	SCC	1	2 MV/m	4.8 cm ϕ	2.6 m

Figure 2-2. Layout of the SNS High Energy Beam Transport (HEBT) beamline taken from the SNS conceptual design.

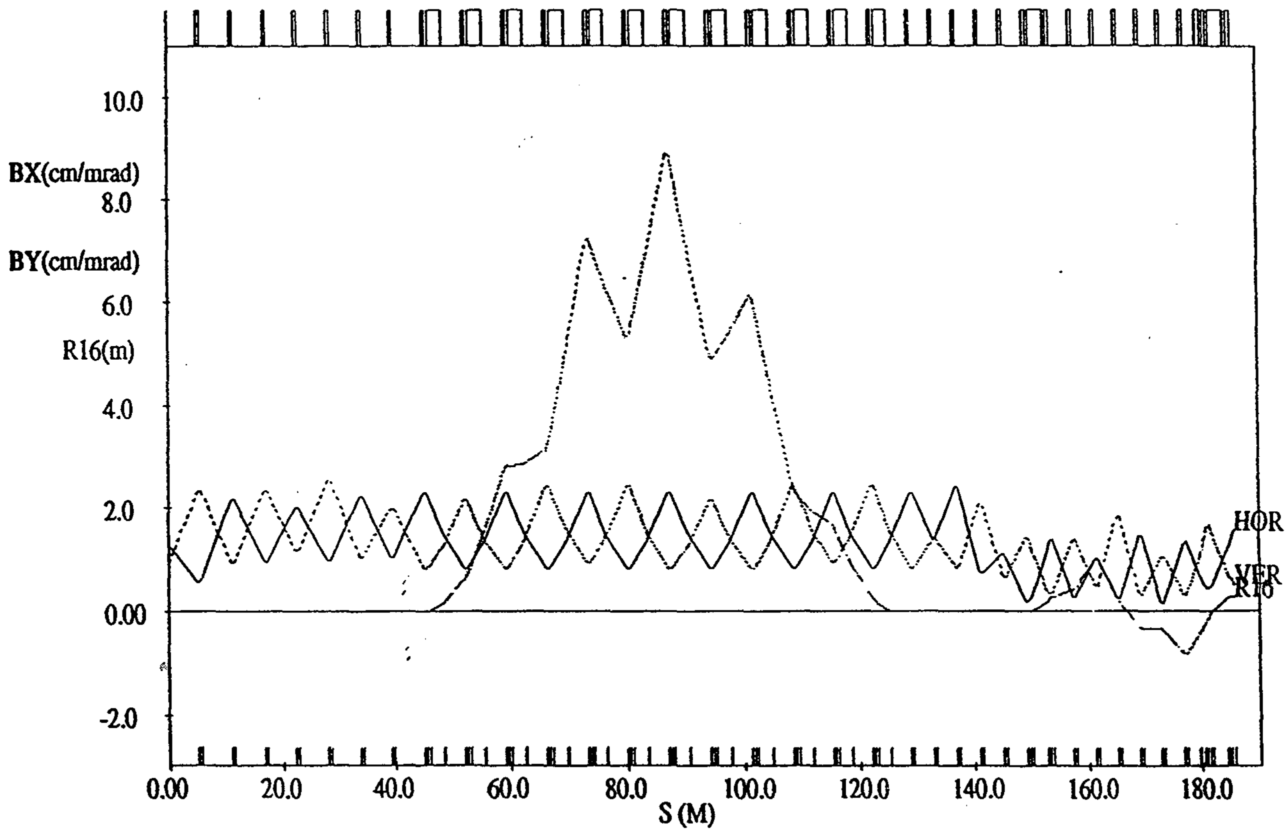

Figure 2-3. Optics parameters for the SNS High Energy Beam Transport (HEBT) beamline taken from the SNS conceptual design.

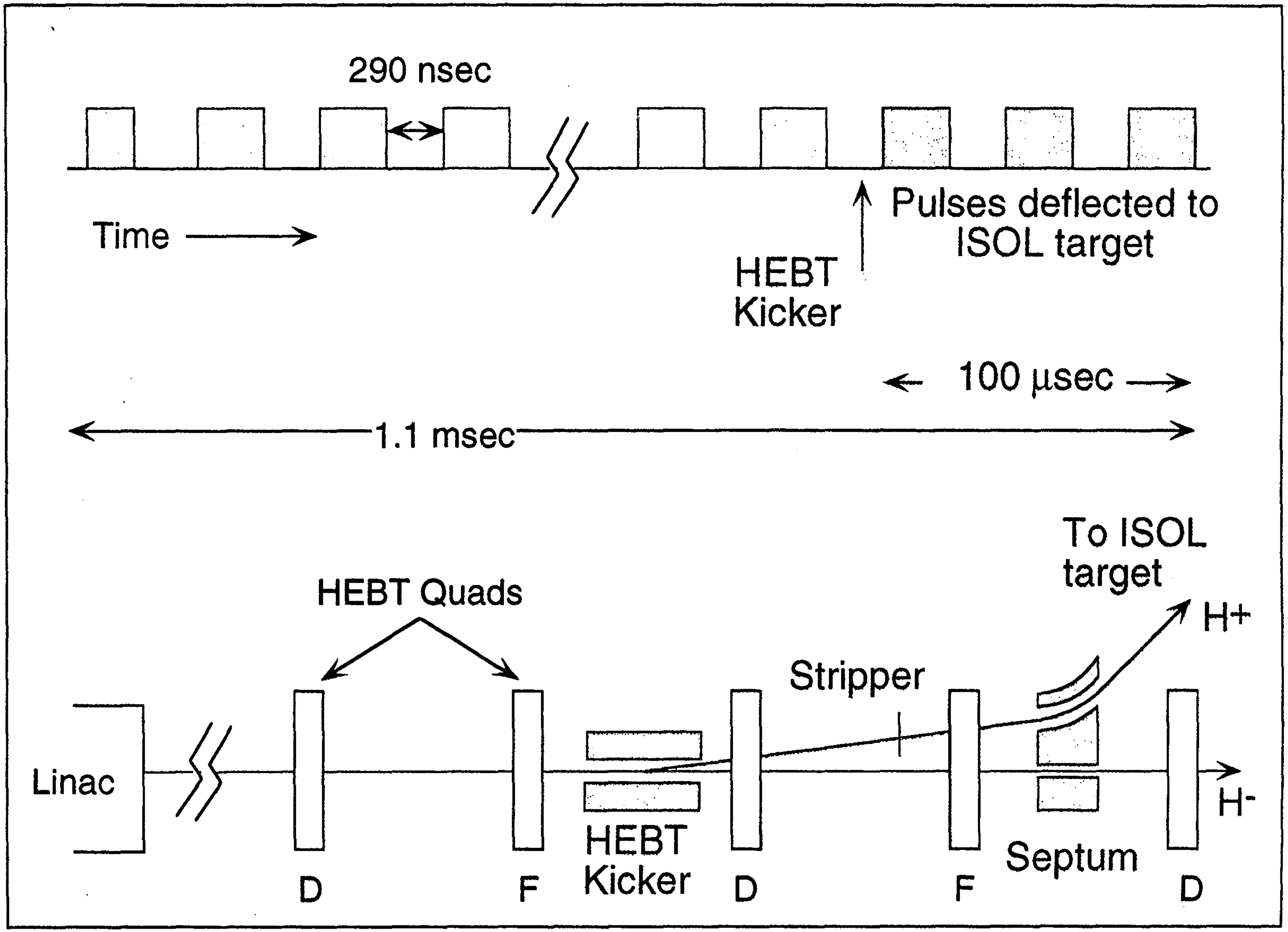

Figure 3-1. Schematic layout of a pickoff scheme based on a fast kicker.

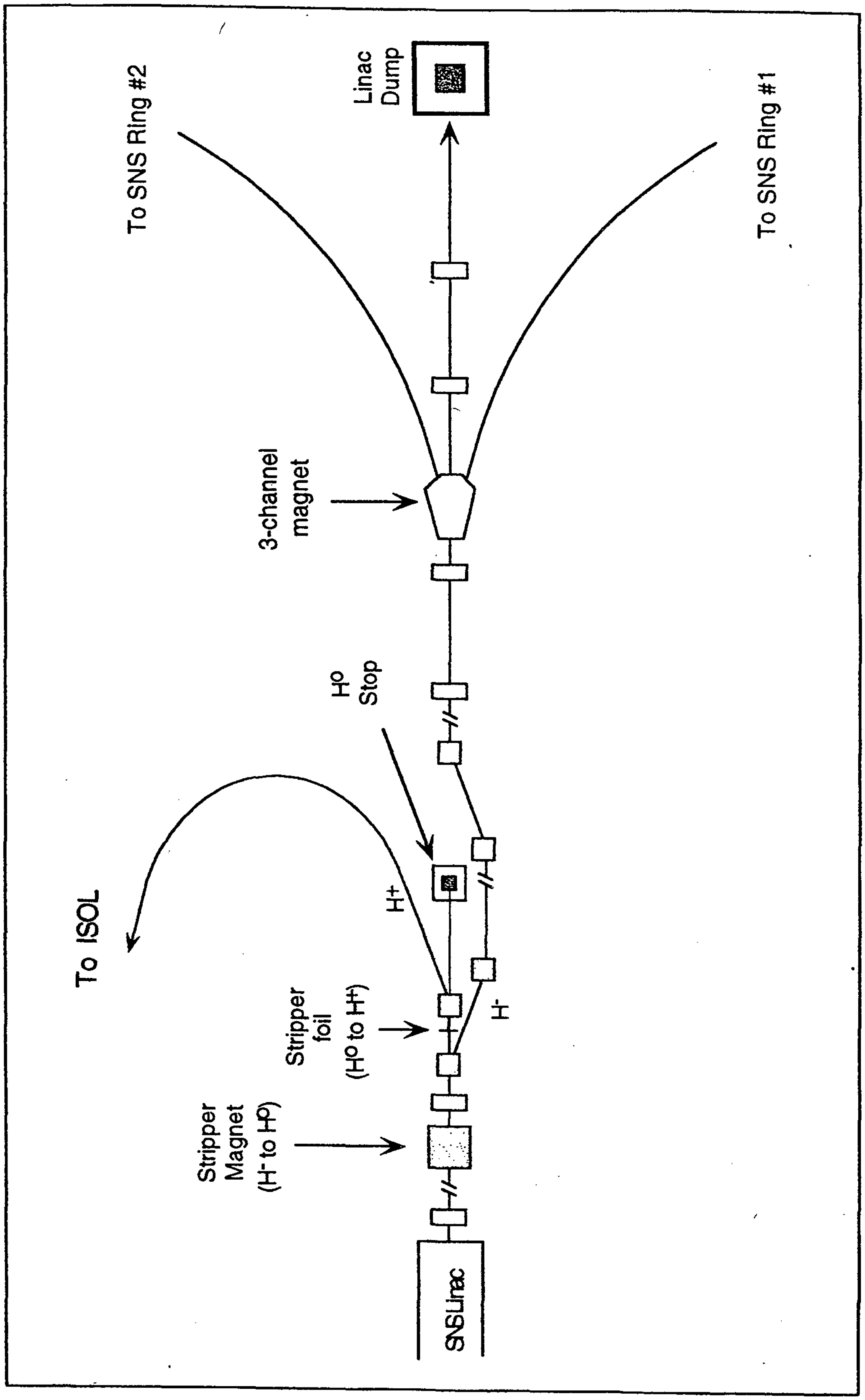

Figure 3-2. Schematic layout of a pickoff scheme based on magnetic stripping.

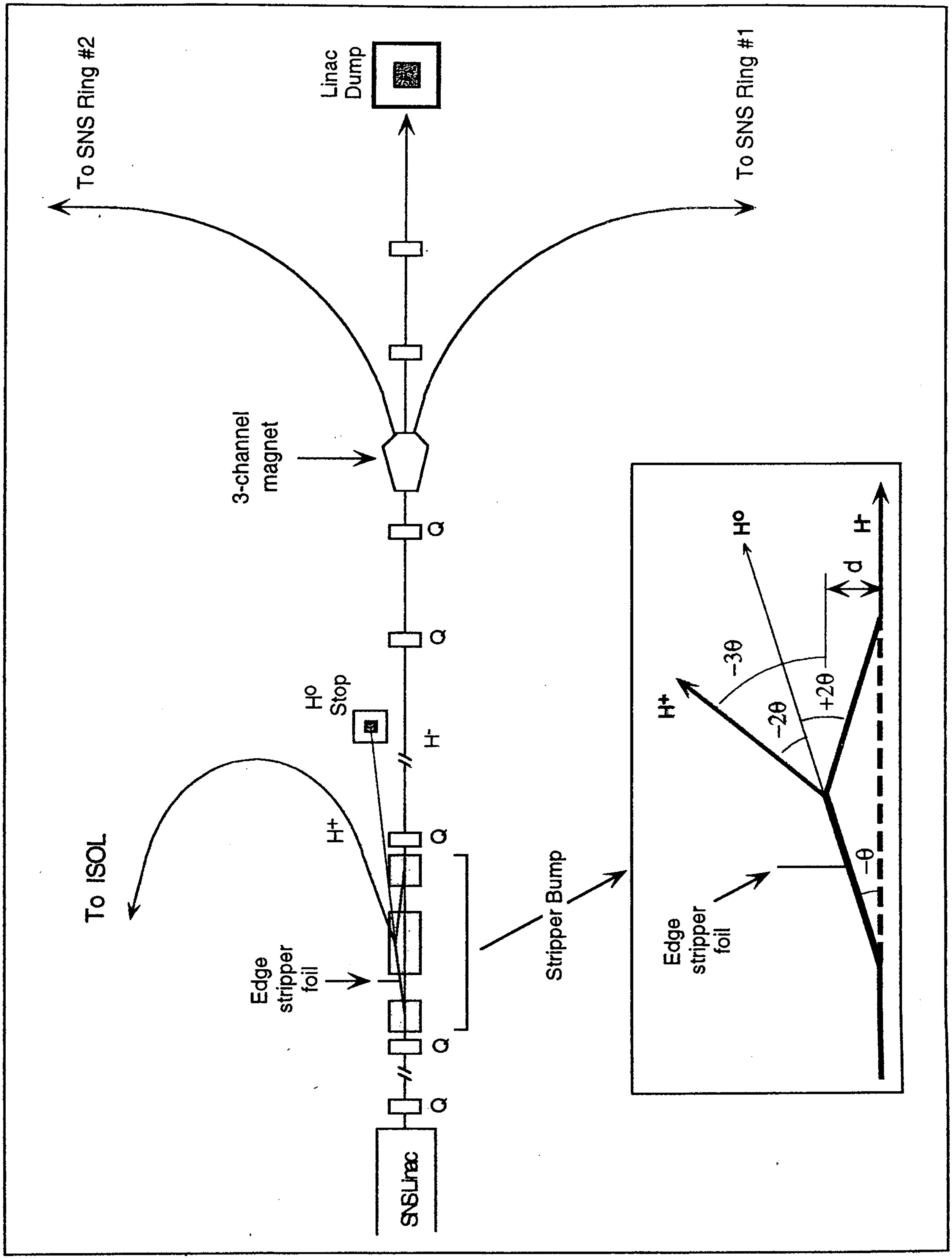

Figure 3-3. Schematic layout of a pickoff scheme based on a stripper foil.

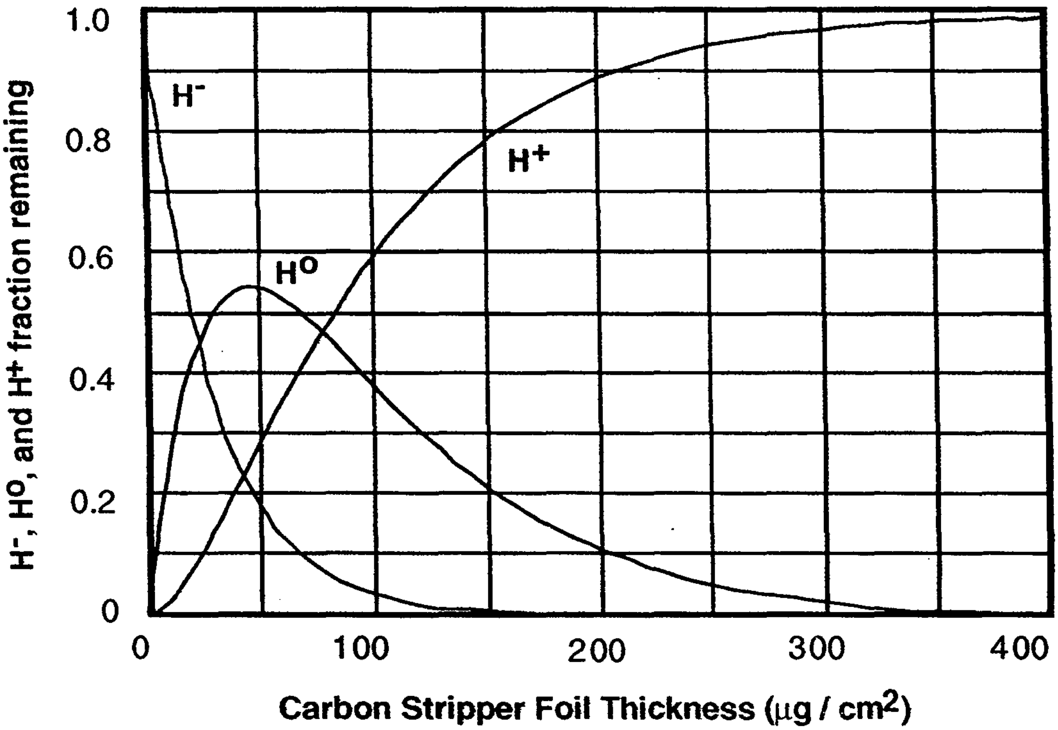

Figure 3-4. Efficiency of carbon foils for stripping a 1 GeV H^- beam.

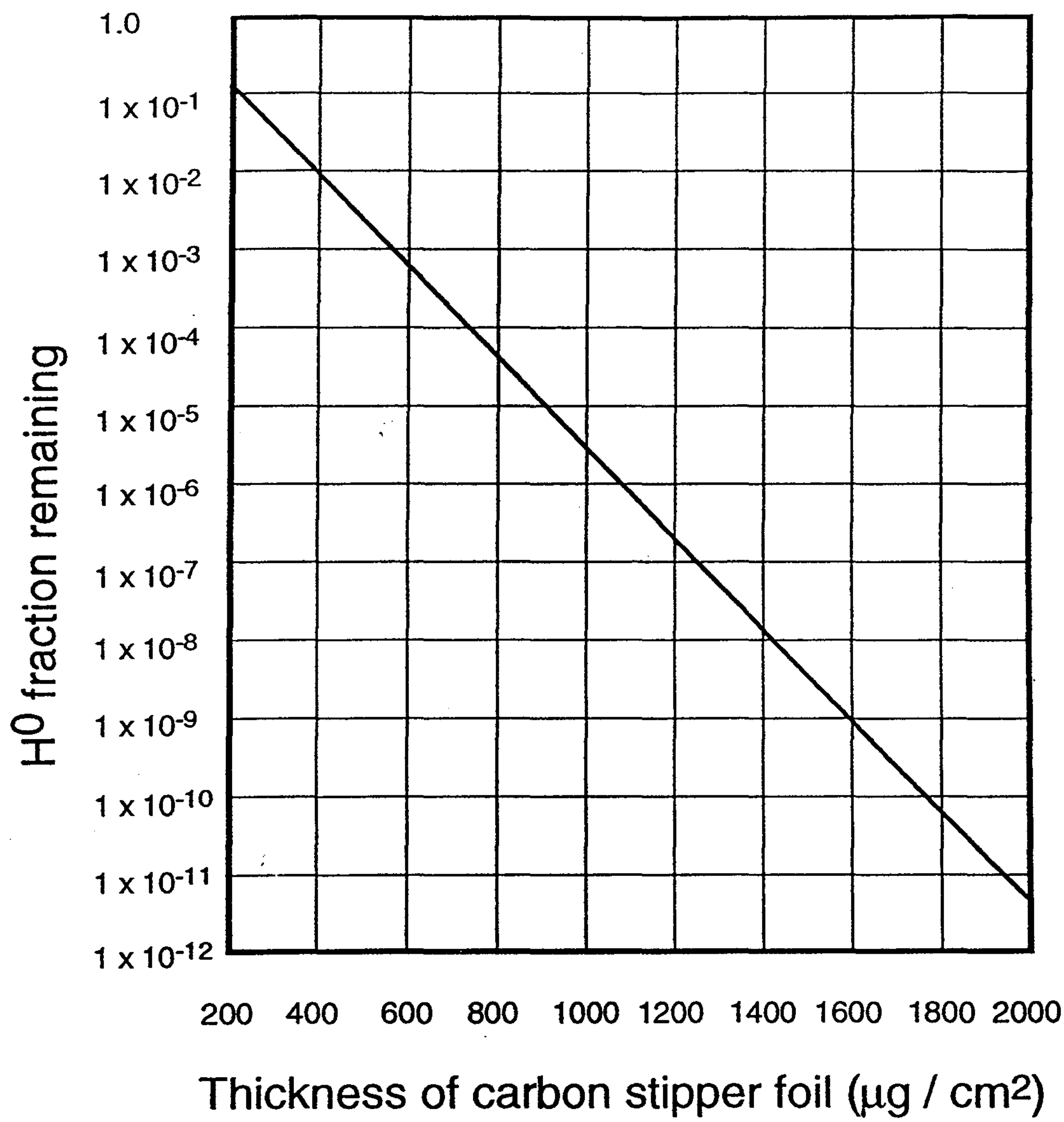

Figure 3-5. Residual production of H^0 for stripping a 1 GeV H^- beam with a thick carbon foil.

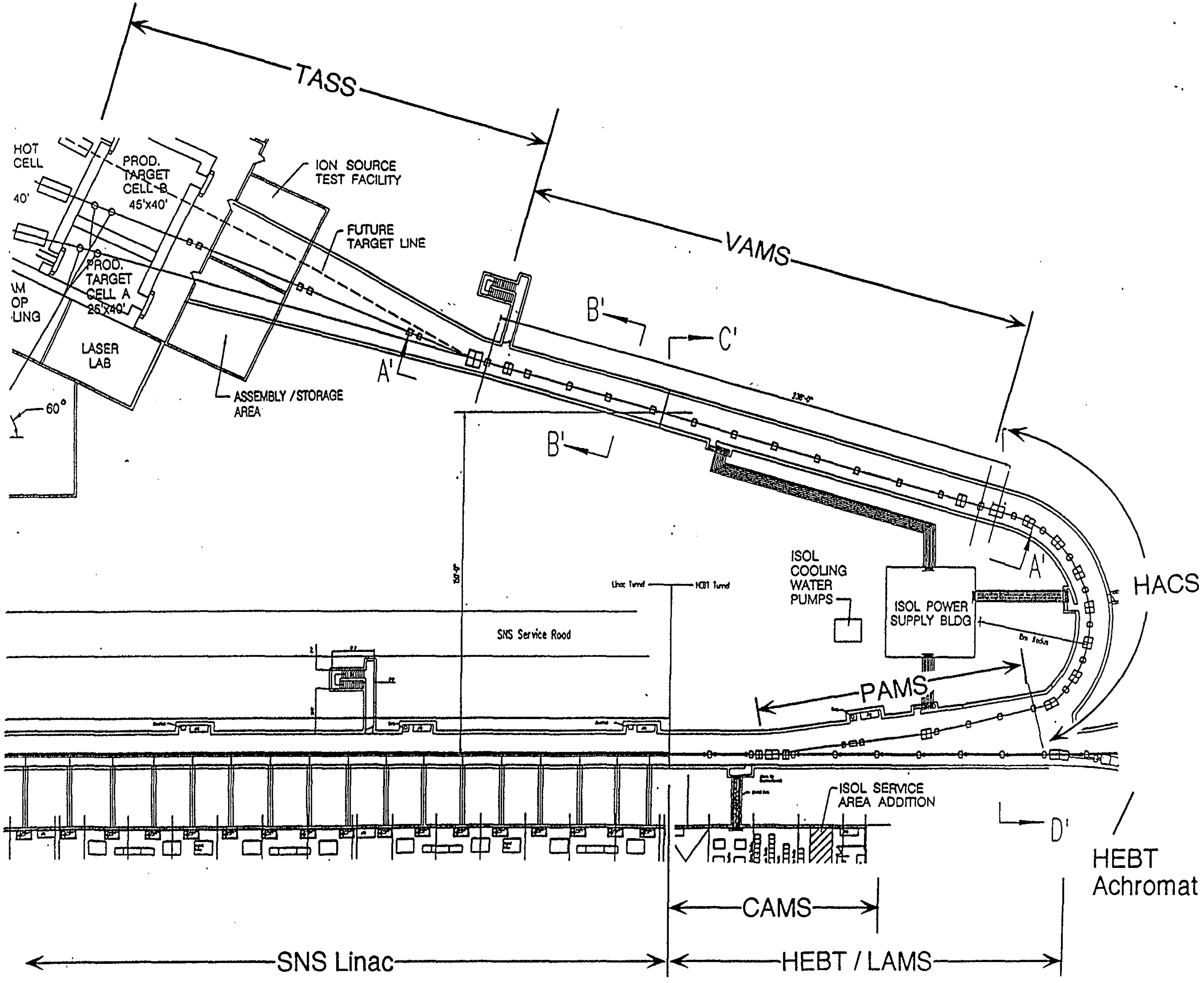

Figure 4-1. Overall layout of proton pickoff and transport line.

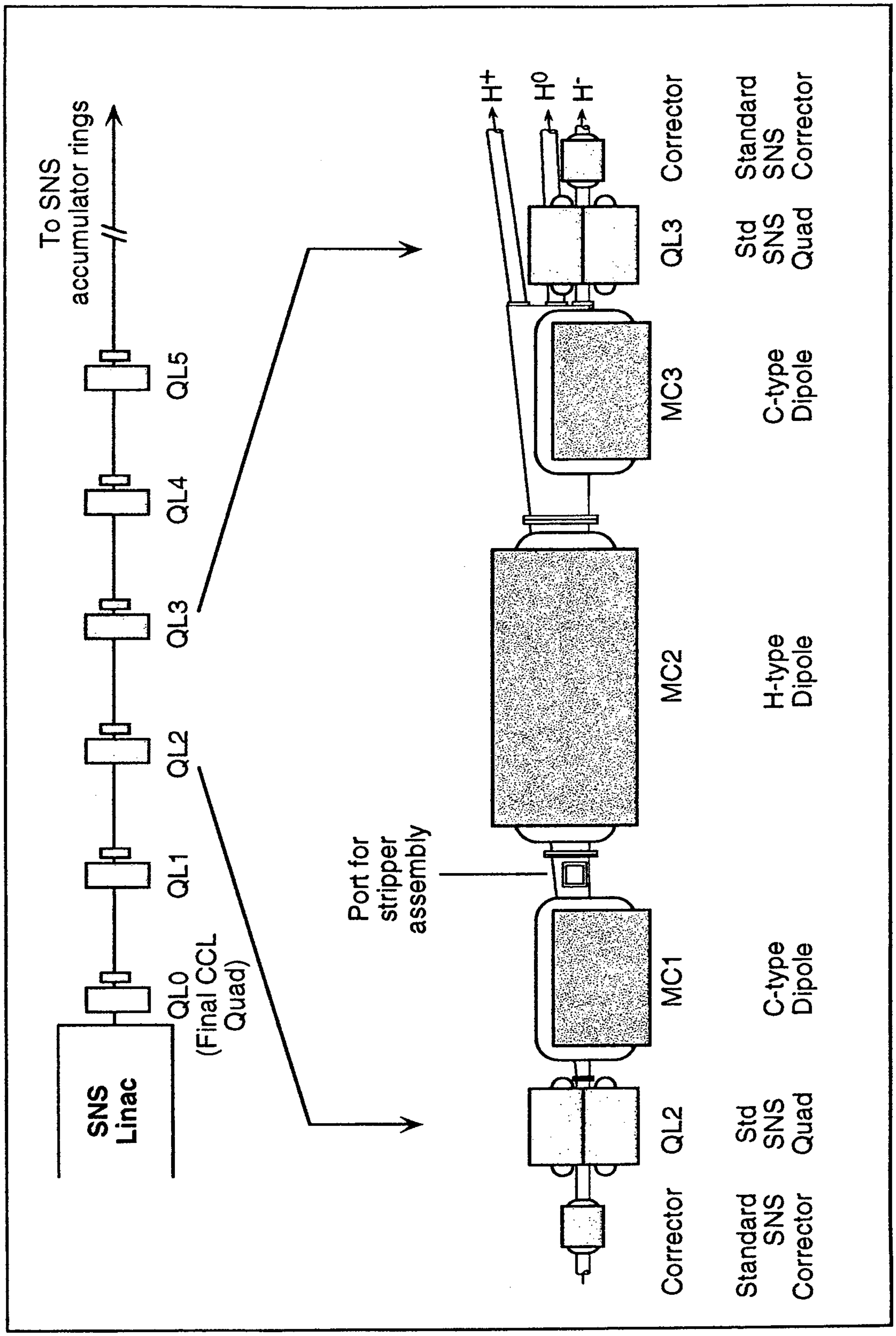

Figure 4-2. Schematic illustration of chicane elements associated with the proton pickoff. A standard SNS 12Q50 quadrupole magnet is shown for QV3. As discussed in section 4.6 of the text, detailed layouts will be required to evaluate possible need for a modified magnet design at this location.

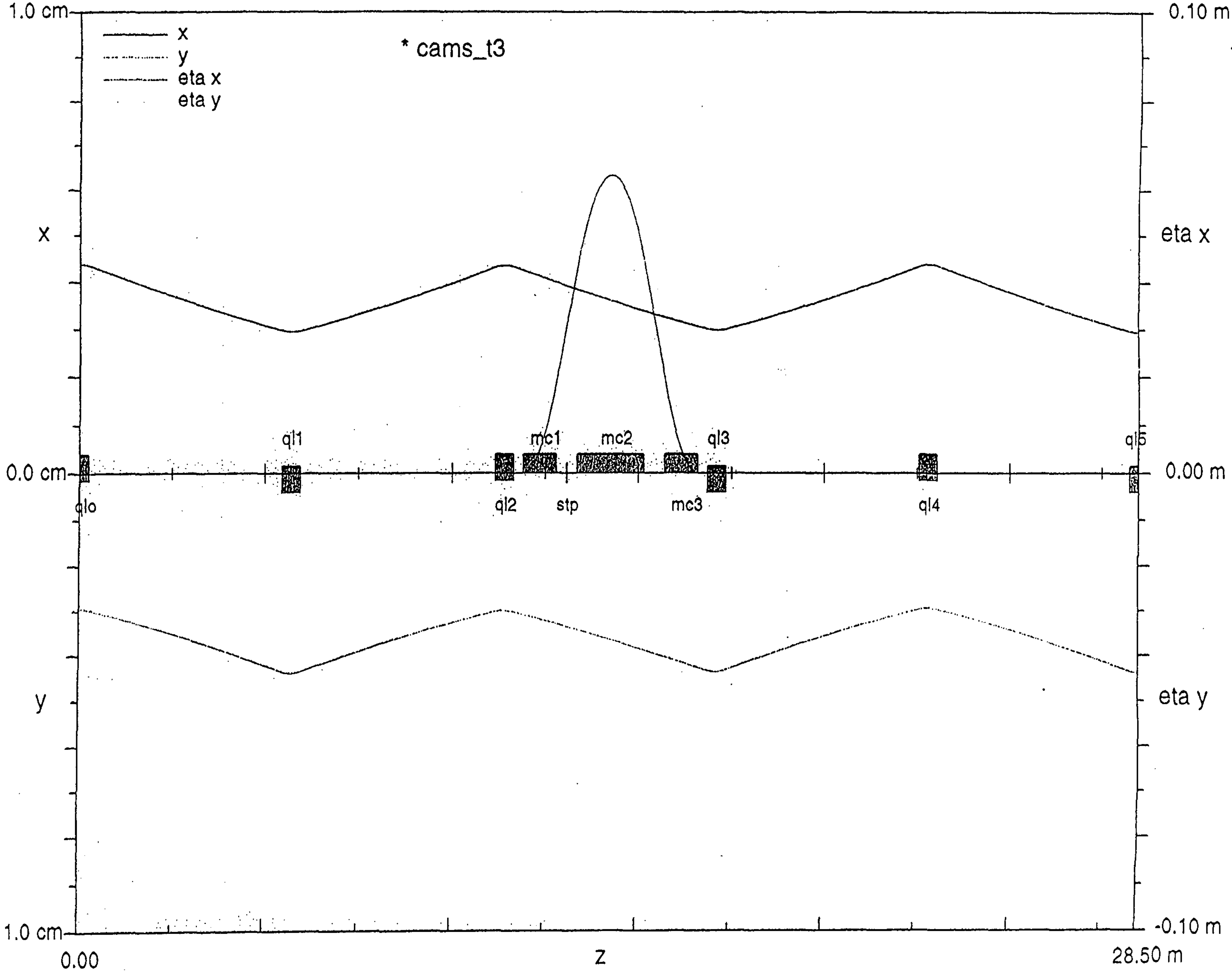

Figure 4-3. Optics parameters for the CAMS beamline.

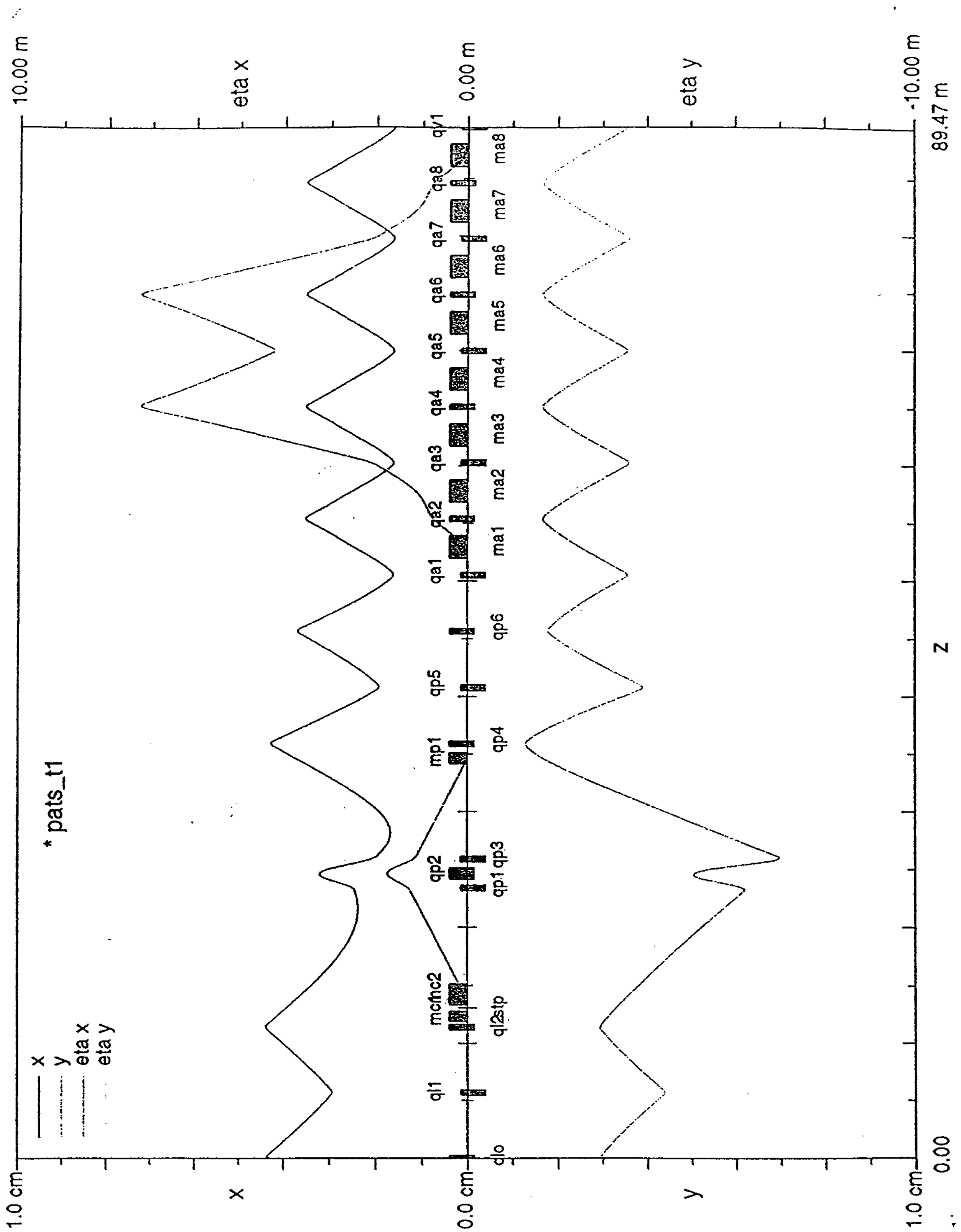

Figure 4-4. Optics parameters for the PAMS and HACS beamlines.

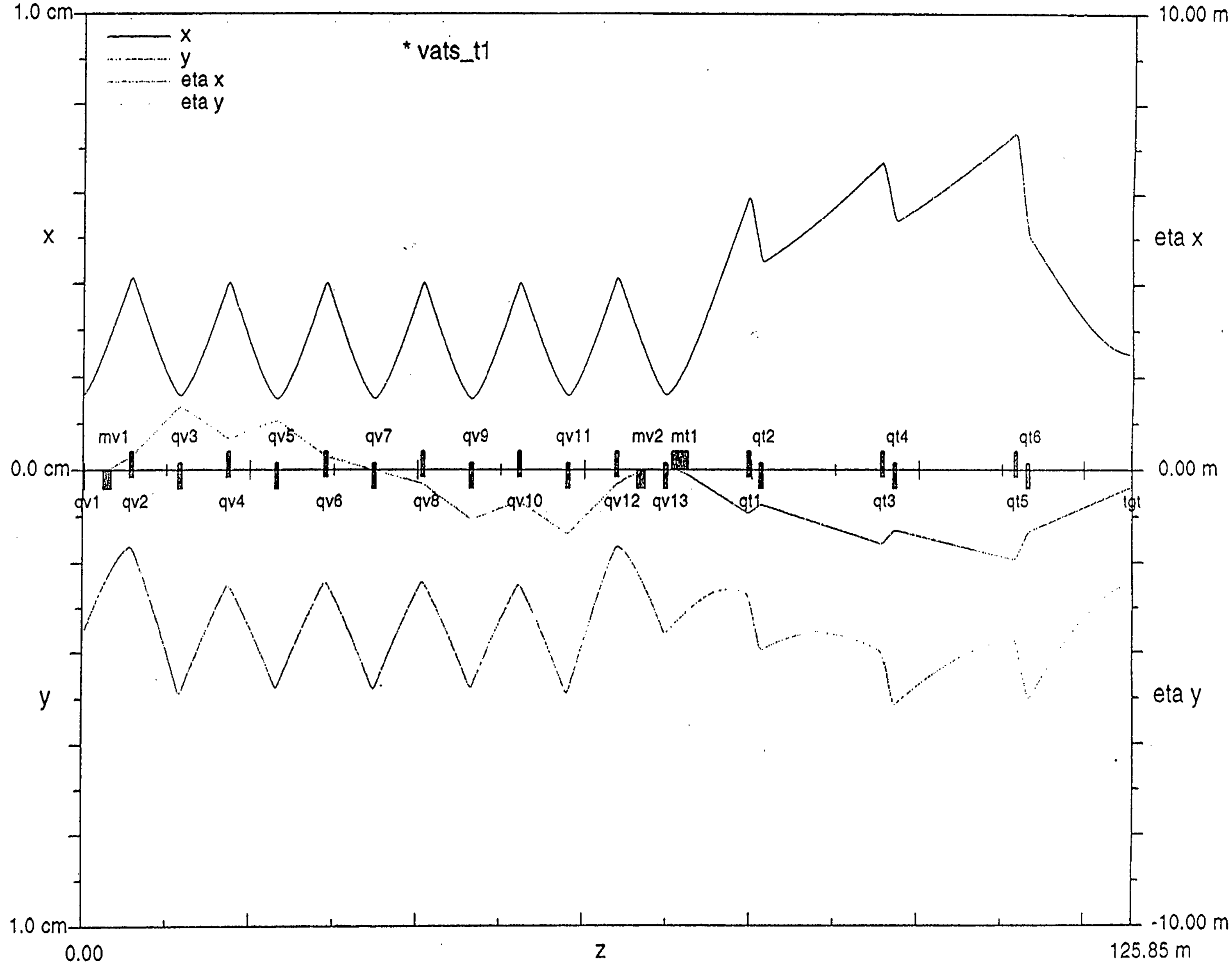

Figure 4-5. Optics parameters for the VAMS and TASS beamlines.

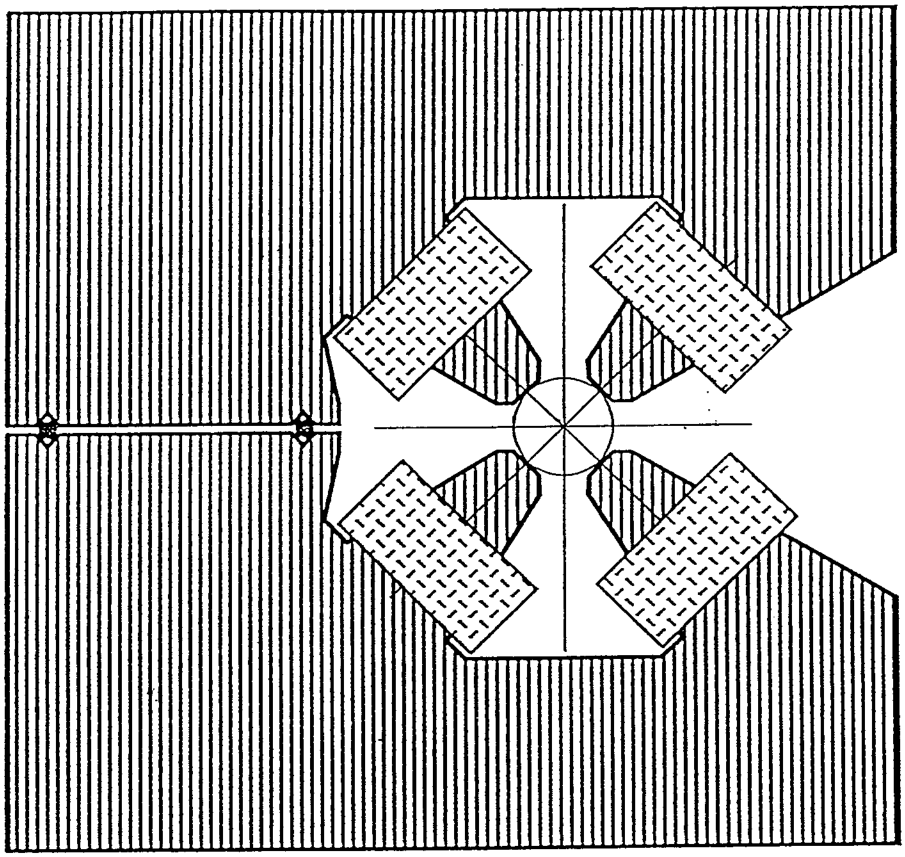

Figure 4-6. Cross section of a C-type quadrupole magnet.

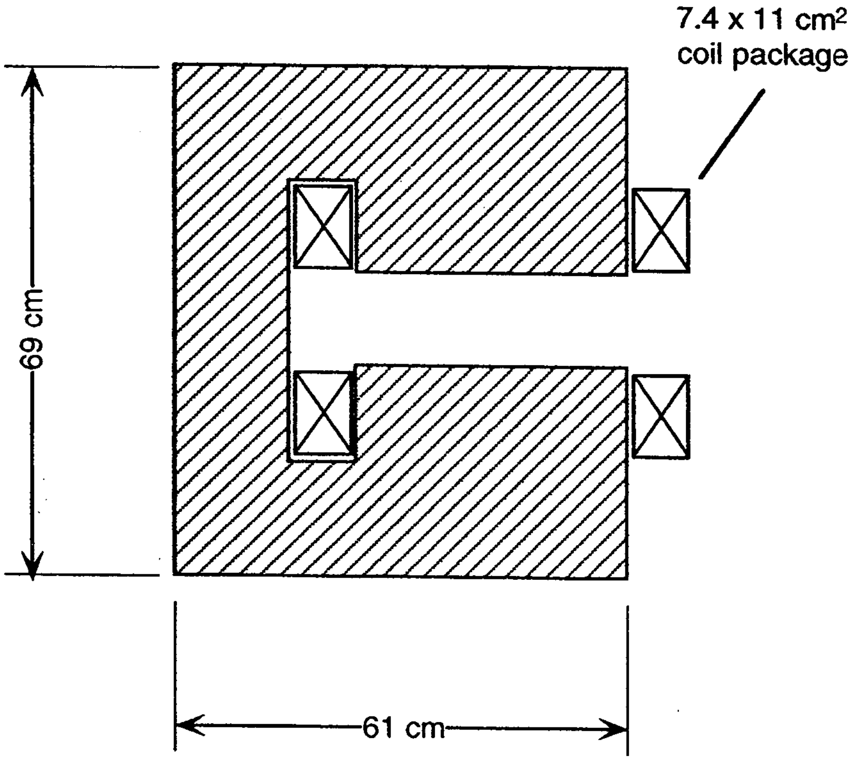

Figure 4-7. Cross section of chicane dipoles MC1, MC3.

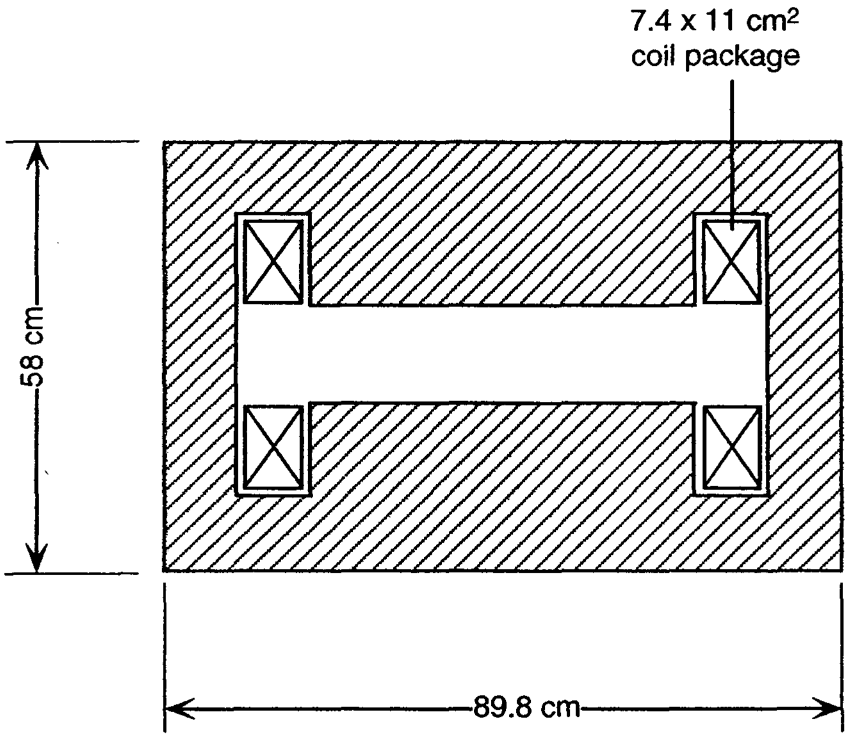

Figure 4-8. Cross section of chicane dipole MC2.

ERNEST ORLANDO LAWRENCE BERKELEY NATIONAL LABORATORY
ONE CYCLOTRON ROAD | BERKELEY, CALIFORNIA 94720

Prepared for the U.S. Department of Energy under Contract No. DE-AC03-76SF00098